Excited States in P^{29} from the Scattering of Protons by Si^{28}†

T. A. Belote, E. Kashy,* and J. R. Risser

Rice University, Houston, Texas

(Received December 28, 1960)

Excited states in P^{29} have been observed by measuring the differential elastic scattering cross section of $Si^{28}(p,p)Si^{28}$ for proton energies from 2.0 to 5.0 Mev and the differential inelastic scattering cross section of $Si^{28}(p,p')Si^{28*}$ ($Q=-1.78$ Mev) for proton energies from 3.0 to 5.2 Mev. Resonances were observed at 2.080, 2.88, 3.095, 3.334, 3.571, 3.710, 3.98, 4.235, 4.36, 4.43, and 4.884 Mev, corresponding to excited states in P^{29} at 4.732, 5.50, 5.711, 5.942, 6.171, 6.305, 6.57, 6.812, 6.93, 7.00, and 7.438 Mev, respectively. Single-level dispersion theory analysis indicates assignments $J^{\pi}=\frac{1}{2}^{+}, \frac{1}{2}^{-}, \frac{5}{2}^{-}, \frac{3}{2}^{+}, \frac{3}{2}^{-}, \frac{1}{2}^{-}, \frac{1}{2}^{+}, \frac{3}{2}^{+}, \frac{1}{2}^{+}, \frac{1}{2}^{-}$, and $\frac{5}{2}^{-}$, respectively, for these states.

ELASTIC scattering of protons from Si^{28} and inelastic scattering to the first excited state of Si^{28} ($Q=-1.78$ Mev[1]; threshold$=1.84$ Mev) were investigated experimentally.[2] The proton energy range extended from 2.0 to 5.0 Mev for the elastic scattering, and from 3.0 to 5.2 Mev for the inelastic. The range 2.0 to 5.2 Mev corresponds to excitation energies from 4.65 to 7.74 Mev in the compound nucleus P^{29*}. To fit the elastic data and make J^{π} assignments to the states in P^{29*} corresponding to the observed resonances, an analysis was made using Wigner single-level dispersion theory. Angular distributions of the inelastically scattered protons were taken and analyzed as a check on the assignments from the elastic scattering analysis. Total inelastic scattering cross sections were also obtained from these angular distributions as a check on the partial widths used in the elastic scattering analysis.

Below 4.78 Mev, the threshold for inelastic scattering to the second excited state of Si^{28} ($Q=-4.61$ Mev), the elastic scattering and the inelastic scattering to the first excited state are the only open particle channels. The partial widths for γ-ray emission are of course negligible compared to the particle widths. Si^{28}, constituting 92.3% of natural silicon, has a 0^{+} ground state and a 2^{+} first excited state. The channel spin in the elastic channel was thus $\frac{1}{2}$; the channel spins in the inelastic channel were $\frac{3}{2}$ and $\frac{5}{2}$.

Considerable work has been done on reactions leading to the same excited states in P^{29}. The $Si^{28}(p,\gamma)P^{29}$ reaction was first studied by Hole, Holtsmark, and Tangen[3] with proton energies from 0.3 to 0.55 Mev. Cohn, Bair, Kington, and Willard[4] observed the γ rays from $Si^{28}(p,p'\gamma)Si^{28}$. They reported resonances at 3.11 Mev ($\Gamma=12$ kev), 3.55 Mev (11 kev), 3.58 Mev (70

kev), 3.71 Mev (40 kev), 4.25 Mev (22 kev), and 4.44 Mev (100 kev). Willard, Bair, Cohn, and Kington[5] reported low intensity resonances in the γ-ray yield at 2.64, 3.88, 3.93, 3.97, and 4.93 Mev, although later measurements[6] showed that the 3.88-Mev resonance was due to Si^{30}.

Val'ter, Malakhov, Sorokin, and Taranov[7] measured and gave an analysis of the elastic scattering for proton energies from 1.5 to 2.2 Mev. They observed resonances at 1.65 Mev ($\Gamma=50$ kev) and 2.08 Mev (14 kev). Their analysis gave $\frac{3}{2}^{-}$ and $\frac{1}{2}^{+}$, respectively, for these states. Sorokin, Val'ter, Malakhov, and Taranov[8] made use of these results for their polarization measurements. Vorona, Olness, Haeberli, and Lewis[9] measured and analyzed the elastic scattering cross section in the energy range from 1.5 to 3.8 Mev. Much of the present work was done before the paper of Vorona *et al.* appeared. Differences in detail between their results and ours in the 2.0- to 3.8-Mev region will be discussed in connection with the assignments at the individual resonances.

Information has recently been obtained on the excited states of P^{29} at higher energies. Okada, Miura, Wakatsuki, and Hirao[10] have reported resonances in $Si^{28}(p,p'\gamma)Si^{28}$ between 4.5 and 5.5 Mev which were not resolved in their experiments. Scattering experiments in the energy range 8 to 9.5 Mev have been reported by Greenlees, Kuo, Lowe, and Petravic[11] and in the range 4.8 to 5.5 Mev by Oda, Takeda, Hu, and Kato.[12]

† Supported in part by the U. S. Atomic Energy Commission.

* Present address: Department of Physics, Massachusetts Institute of Technology, Cambridge, Massachusetts.

[1] The properties of the ground and first excited state of Si^{28} and the binding energy of a proton added to form P^{29} were taken from the review article of P. M. Endt and C. M. Braams, Revs. Modern Phys. **29**, 683 (1957).

[2] T. A. Belote, E. Kashy, and J. R. Risser, Bull. Am. Phys. Soc. **5**, 108 (1960).

[3] N. Hole, J. Holtsmark, and R. Tangen, Z. Physik **118**, 48 (1941).

[4] H. O. Cohn, J. K. Bair, J. D. Kington, and H. B. Willard, Phys. Rev. **99**, 644(A) (1955).

[5] H. B. Willard, J. K. Bair, H. O. Cohn, and J. D. Kington, Bull. Am. Soc. **1**, 264 (1956).

[6] A. C. L. Barnard, S. Bashkin, C. Broude, and C. E. Hornbach, Bull. Am. Phys. Soc. **5**, 56 (1960).

[7] A. K. Val'ter, I. I. Malakhov, P. V. Sorokin, and A. I. Taranov, Izvest. Akad. Nauk S.S.S.R. Ser. Fiz. **22**, 871 (1958) [translation: Bull. Acad. Sciences U.S.S.R. **22**, 865 (1958)].

[8] P. V. Sorokin, A. K. Val'ter, I. I. Malakhov, and A. I. Taranov, J. Exptl. Theoret. Phys. U.S.S.R. **35**, 1386 (1959) [translation: Soviet Phys.—JETP **35**(8), 969 (1959)].

[9] J. Vorona, J. W. Olness, W. Haeberli, and H. W. Lewis, Phys. Rev. **116**, 1563 (1959).

[10] E. Okada, I. Miura, T. Wakatsuki, and Y. Hirao, J. Phys. Soc. Japan **13**, 541 (1958).

[11] G. W. Greenlees, L. G. Kuo, J. Lowe, and M. Petravic, Proc. Phys. Soc. (London) **71**, 347 (1958).

[12] Y. Oda, M. Takeda, C. Hu, and S. Kato, J. Phys. Soc. Japan **14**, 1255 (1959).

EXPERIMENTAL PROCEDURE

The scattering chamber, which was designed for the use of thin self-supporting foils as targets,[13] has been previously described.[14] The chamber consisted of two shallow cylinders. The fixed lower cylinder contained the beam defining slits, Faraday cup, and target holder; the movable upper cylinder contained the detectors and associated slit systems. The detectors were 0.025-inch thick CsI(Th) crystals on Dumont-6291 photomultiplier tubes. The over-all accuracy of the angle of scattering was estimated to be ±0.5° from a calibration check on the chamber using Rutherford scattering from Au.

The chamber was fitted with two counters spaced at 90° in ϕ, the angle about the chamber axis of rotation.[14] This in part explains the choice of angles in taking data. The elastic data were taken at two sets of angles: (1) the backward counter was set at 125.3° c.m., the forward counter then being at 38.9° c.m.; (2) the forward counter was set at 90.0° c.m., the backward counter then being at 165.1° c.m. Considerable advantage is experienced in taking elastic data simultaneously at two angles because the relative positioning of the anomalies due to a resonance can be determined with greater precision than in repeat runs with one counter. Relative calibration of the counters was to better than 1%. The inelastic data were taken at 88.0° and 164.8° (laboratory) with a 256-channel analyzer. With a complete pulse-height distribution in the neighborhood of the inealstic peak, it was possible to estimate background and subtract it. There was never any appreciable background in the elastic channel. The elastic data were taken with a single-channel analyzer. A 20-channel analyzer was operated continuously in parallel with the single channel to check the positioning of the elastic group in the latter.

The Rice University 5.5-Mev Van de Graaff accelerator was used to accelerate the protons. The proton energy was selected by the slit system of the 90° analyzing magnet. The magnetic field was set to the frequency of the proton-moment magnetometer. The Li⁷(p,n)Be⁷ neutron threshold was used as the calibration point. The uncertainty in proton energy is believed to be less than ±5 kev below 4 Mev and to be less than ±10 kev at 5 Mev.

The targets were of natural silicon (92.3% Si²⁸). Both Si metal and SiO foils were used. The method of preparation was the same as previously described for carbon foils.[13] Si and SiO were both deposited by evaporation onto 0.00025-inch nickel foil. Carbon was the only filament material found to survive contact with Si metal at the high evaporation temperatures. Si was therefore evaporated from heavy boat-shaped carbon filaments. Tantalum was used for the SiO. SiO

targets proved considerably less fragile under proton bombardment than Si and were used when possible. A single Si target 32 μg/cm² thick (3.7 kev at 3 Mev) was used in taking most of the elastic scattering data. A 60.3-μg/cm² (7.0 kev at 3 Mev) Si target was used to take the elastic scattering data in the region of the 2.08-Mev resonance at 90° and 165°. The excitation curves of the inelastically scattered protons were taken with a 39.2-μg/cm² (4.5 kev at 3 Mev) Si target from 3.0 to 3.8 Mev and with a 25.6-μg/cm² (2.95 kev at 3 Mev) Si target from 3.8 Mev to 5.2 Mev. A SiO target 178 μg/cm² thick (21.8 kev at 3 Mev) was used in taking the angular distributions of the inelastically scattered protons.

The absolute cross-section scale was determined in the following way. It was not possible to make an absolute determination of target thickness by weighing. Therefore the thickness of a standard target was determined from the Rutherford cross section of Si for protons between 1 and 2 Mev by measuring the elastic scattering in that range at a number of angles and energies at which the total cross section could legitimately be assumed to be equal to the Rutherford cross section. The elastic scattering cross section at 3.2 Mev and 165° c.m. was then determined to be 90.0 millibarns/steradian using this standard target. This cross-section value is believed determined to within ±3% by this procedure. All target thicknesses were determined by counting elastically scattered protons at 3.2 Mev and 165° c.m. using 90.0 mb/steradian as the cross section. 3.2 Mev and 165° c.m. were picked because the elastic scattering counting rate there was known to be insensitive to fluctuations in energy and small errors in setting the angle.

The cross sections given throughout the paper are referred to Si²⁸ by multiplying the number of atoms in the standard target as determined from the Rutherford cross section by a factor 0.923 before calculating the cross section to be 90.0 mb/steradian at 3.2 Mev and 165° c.m. The standard cross section is thus based on the number of Si²⁸ atoms in the target as though the others did not exist. This convention has the effect of giving correctly the heights of the resonances due to Si²⁸ but introduces errors of the order of 8% in the background cross sections. There is, however, no way of correcting the background for the contributions of Si²⁹ and Si³⁰. In the following paragraph the errors will be discussed as if this systematic error due to the presence of Si²⁹ and Si³⁰ did not exist.

Taking into account statistical errors in counting, errors due to imperfect chamber geometry, errors in charge integration, and the like, errors in the relative elastic scattering cross sections are estimated less than ±5%. Because background had to be subtracted from the inelastic scattering data the errors are somewhat higher, but the relative cross sections over the resonances are estimated to be within ±8%. Where the inelastic scattering cross section is of the order of a

[13] E. Kashy, R. R. Perry, and J. R. Risser, Nuclear Instr. and Methods 4, 167 (1959).

[14] E. Kashy, R. R. Perry, and J. R. Risser, Phys. Rev. 117, 1289 (1960).

millibarn/steradian, as for example at 4 Mev, the uncertainty is of the order of $\pm 20\%$, due to statistical and background subtraction errors. Excluding the errors due to isotopic impurity, absolute cross sections are believed accurate to $\pm 10\%$ in the elastic scattering and $\pm 12\%$ in the inelastic scattering.

ANALYSIS

Elastic Scattering

The form of the scattering matrix[15] was taken from single-level dispersion theory. While the data indicated a number of broad interfering resonances with narrow ones superimposed, it was nevertheless hoped that the single-level approximation would be valid enough to yield reasonably precise parameters for the corresponding states. The following form of the differential elastic scattering cross section for channel spin $\frac{1}{2}$ was used:

$$d\sigma(\theta)/d\Omega = |A|^2 + |B|^2, \qquad (1)$$

where

$$A = -\frac{n}{2k} \csc^2(\theta/2) \exp[i\eta \ln \csc^2(\theta/2)]$$

$$+ \frac{(4\pi)^{\frac{1}{2}}}{k} \sum_l (2l+1)^{\frac{1}{2}} e^{i(2\alpha_l + \phi_l)} \sin\phi_l Y_l^0(\theta)$$

$$+ \frac{i\sqrt{\pi}}{k} \sum_l \frac{1}{(2l+1)^{\frac{1}{2}}} [(l+1)K_l^+ + lK_l^-] Y_l^0(\theta),$$

$$B = \frac{i\sqrt{\pi}}{k} \sum_l \left[\frac{l(l+1)}{2l+1} \right]^{\frac{1}{2}} [K_l^+ - K_l^-] Y_l^1(\theta),$$

$$K_l^\pm = e^{2i(\alpha_l + \phi_l)} \sum_{J\pi} \frac{\Gamma_l^{J\pi}}{\Gamma^{J\pi}} [1 - \exp(2i\beta^{J\pi})] \delta_{J, l \pm \frac{1}{2}},$$

and

$$\beta^{J\pi} = \tan^{-1} \left[\frac{\Gamma^{J\pi}/2}{E_0^{J\pi} - E} \right].$$

In this expression, $\alpha_l = \sigma_l - \sigma_0$ and

$$\phi_l = \xi_l - \sigma_l = -\tan^{-1}(F_l/G_l)$$

in the notation of Blatt and Weisskopf,[16] k is the wave number, η is the Coulomb field parameter $14e^2/\hbar v$ for protons on Si, $\Gamma^{J\pi}$ is the total width (laboratory) of a resonance due to the state J^π at resonance energy $E_0^{J\pi}$, and $\Gamma_l^{J\pi}$ is the partial elastic scattering proton width. In fitting the elastic scattering data, the "hard-sphere phases" ϕ_l were allowed to deviate somewhat from the tabulated values of $-\tan^{-1}(F_l/G_l)$. The values of the ϕ_l actually used in the elastic scattering fit between 2.0 and 5.0 Mev are plotted in Fig. 1. While

[15] J. M. Blatt and L. C. Biedenharn, Revs. Modern Phys. **24**, 258 (1952).

[16] J. M. Blatt and V. F. Weisskopf, *Theoretical Nuclear Physics* (John Wiley & Sons, Inc., New York, 1952), pp. 330–333.

it is necessary to use the complete designation $\Gamma_l^{J\pi}$ for the elastic scattering proton partial widths in Eq. (1), the simpler designation Γ_p will be used generally instead of $\Gamma_l^{J\pi}$, both in tables that list parameters of individual resonances, where the indices J, π, and l can be dropped without creating ambiguity, and in most of the discussions of individual resonances which follow.

Equation (1) was programmed for the IBM-704 computer. Provision was made in the program for the parameters of 20 possible resonances corresponding to each J^π value up to $9/2^+ (l \leqslant 4)$. A resonance was included by specifying its $\Gamma^{J\pi}$, $\Gamma_l^{J\pi}$, and $E_0^{J\pi}$. After inserting these parameters, the behavior of the resonance was obtained from the variation of $\beta^{J\pi}$. In order to reduce the number of starting J^π possibilities to be used in computing fits to the experimental data, isolated single-level resonance curves for the differential cross section were computed at 2.3 Mev for all J made with $l = 0$ to 3. The ϕ_l were all taken equal to zero. These single-level curves are shown in Fig. 2. By comparing these calculated resonance shapes with those observed in the experimental data, the assignments to the experimental data at each resonance could be restricted to at most two or three J^π possibilities. Computations were then carried out starting with these possibilities. For promising J^π assignments, the relative elastic scattering widths $\Gamma_l^{J\pi}/\Gamma^{J\pi}$ were varied until best agreement was obtained between data and theory.

Inelastic Scattering

The analysis consisted in making least-squares fits to the experimental inelastic scattering angular distributions and then obtaining theoretical angular distributions to match the least-squares fits using Eq. (3.16), (4.5), and (4.6) of Blatt and Biedenharn.[16] Since the first excited state of Si^{28} is a 2^+ state, the
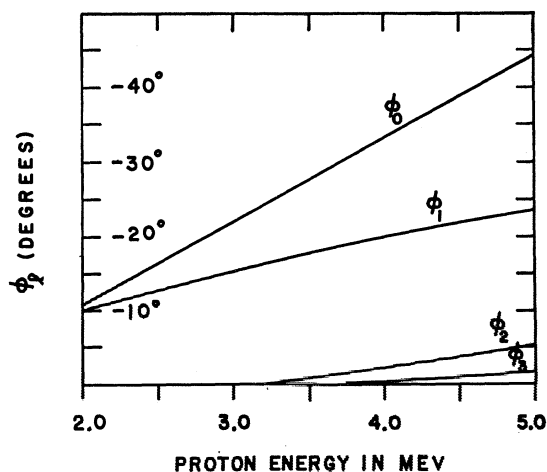

FIG. 1. Values of ϕ_l used in the fits to the elastic scattering data between 2.0 and 5.0 Mev.
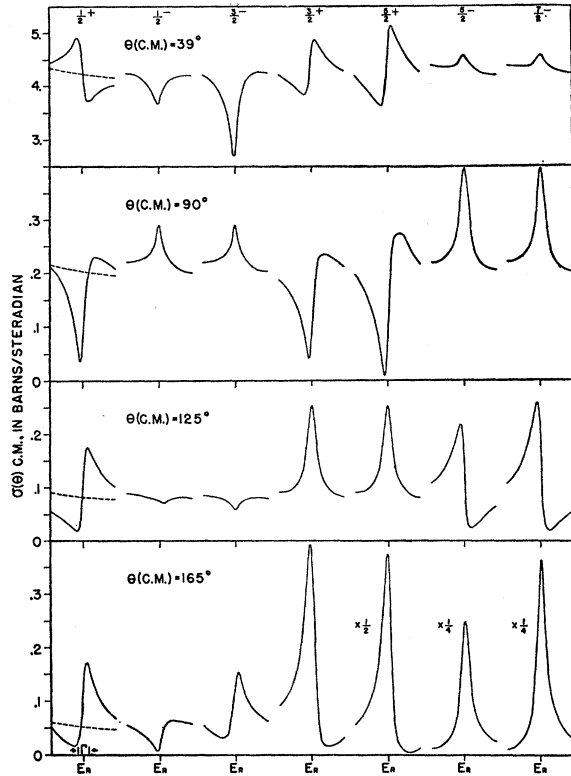
Fig. 2. Theoretical single level resonance shapes for Si^{28}(p,p)Si^{28} at $E_0{}^{J\pi}=2.3$ Mev for all the values of J^π formed with l equal to 3 or less. All the ϕ_l were taken equal to zero.

inelastic protons have channel spins $\frac{3}{2}$ and $\frac{5}{2}$. The theoretical angular distributions are sensitive to the channel spin mixture, so that fits to the experimental distributions can have significance in connection with the elastic scattering analysis but are not capable of removing all ambiguities. As an interesting example, the $\frac{1}{2}^+$, $\frac{3}{2}^+$, and $\frac{5}{2}^+$ states can yield the same angular distributions, namely isotropic, because l' can be zero when $S'=J$ in the latter two cases. In the case of an isolated resonance the procedure consisted in computing theoretical angular distributions for $S'=\frac{3}{2}$ and $\frac{5}{2}$ separately using only the lowest allowed l' value with each S'. The theoretical distributions were then mixed in the correct proportions to match the least-squares distribution. In the case of interference, combinations of channel spins were tried each with the lowest allowed l' value. Restriction to the lowest l' appears to be a valid approximation in the energy range of these experiments since the penetrability factors $A_{l'}{}^2$ are quite large for $l'>1$ even at 5-Mev incident energy. The inelastic scattering analysis was in fact successful in resolving several ambiguities left in the assignments by the elastic scattering analysis, as will be brought out in the discussions of the individual resonances. It is also interesting that no resonance requiring $l'\gtrsim 2$ was found in the inelastic scattering data in the energy range of these experiments. Two $\frac{1}{2}^+$ states (smallest $l'=2$) which

produced strong resonances at 3.98 and 4.36 Mev in the elastic scattering cross section could not be detected in the inelastic.

The experimental angular distributions were taken on resonance. On resonance the theoretical angular distribution due to an isolated state in the above approximation simplifies to

$$\frac{d\sigma(\theta)}{d\Omega}=\frac{1}{2k^2}\frac{\Gamma_p\Gamma_{p'}}{\Gamma^2}\sum_L\sum_{S'}(-)^{S-S'}\frac{\Gamma_{l'S'}}{\Gamma_{p'}}$$
$$\times Z(lJlJ,SL)Z(l'Jl'J,S'L)P_L(\cos\theta),\quad(2)$$

where only one l' is associated with each S'. $\Gamma_p[=\Gamma_l{}^{J\pi}$ of Eq. (1)] is the elastic scattering proton partial width. $\Gamma_{p'}$ is the inelastic scattering proton partial width for decay via both S' channels. $\Gamma_{l'S'}$ is the inelastic scattering partial width for decay via the channel S' with orbital angular momentum l'. As previously used, l, k, and S refer to the orbital angular momentum, wave number, and channel spin in the incident proton channel. For the expression used in the case of interference between resonances, reference is made to a previous paper[14] by two of us.

RESULTS

The experimental differential elastic scattering cross sections measured at c.m. angles 39°, 90°, 125°, and 165° from 2.0 to 5.0 Mev are shown in Fig. 3. The cross sections are in the center-of-mass system, while the energies are laboratory bombarding energies at the center of the target. The solid lines are fits obtained from the IBM-704 computer using Eq. (1). Figure 4 shows the differential inelastic scattering cross sections at laboratory angles 88° and 165° from 3.0 to 5.2 Mev. In Fig. 4 the curves are drawn through the experimental points. The scales specify c.m. cross sections and laboratory bombarding energies at the center of the target. The parameters of the resonances as obtained from the elastic and inelastic scattering data and as used in the final fit of Fig. 3 to the elastic scattering data are listed in Table I. Resonances were observed at 2.080, 2.88, 3.095, 3.334, 3.571, 3.710, 3.98, 4.235, 4.36, 4.43, and 4.884 Mev. As shown in the table, the parameters of two resonances outside the 2.0- to 5.0-Mev interval were included in the input data to the IBM 704 in order to improve the fit at the ends of the interval: $\frac{3}{2}^-$ at 1.660 Mev[7,9] and a broad resonance with $J^\pi=\frac{1}{2}^+$ at 5.4 Mev suggested by the work[10,12] above 5 Mev. The fit of Fig. 3 is slightly improved above 2 Mev and significantly improved between 4.5 and 5.0 Mev by the inclusion of these states. The assignments and widths will be discussed for the resonances individually in the paragraphs immediately following.

Limits of error are explicitly stated in Table I for only a few entries. Unless explicitly stated or implied by the number of significant figures, the resonance energies are believed correct to within ±5 kev, except
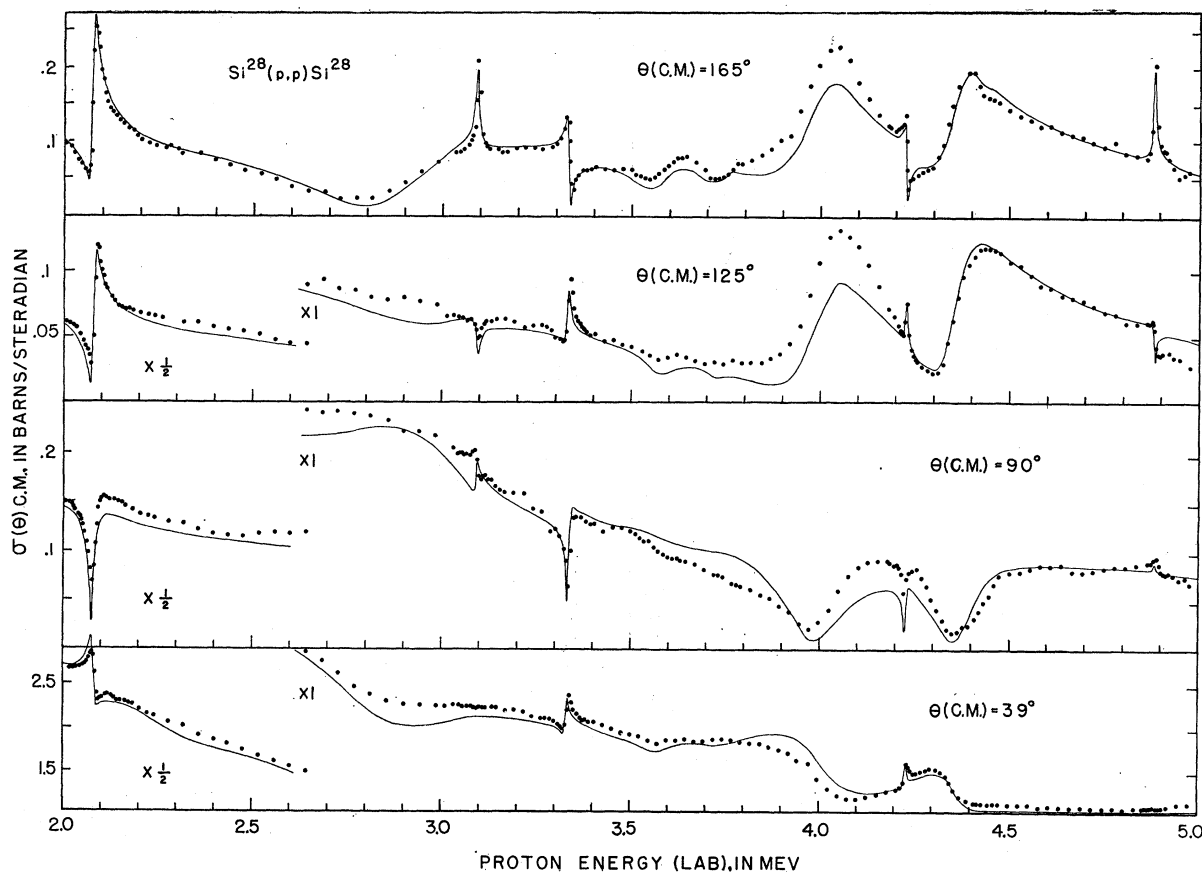
FIG. 3. The differential elastic c.m. scattering cross section at c.m. angles 39°, 90°, 125°, and 165° from 2.0 to 5.0 Mev. The curves are computed from Eq. (1) with the parameters listed in Table I and with the ϕ_l plotted in Fig. 1. The limits of error in the cross sections are discussed in the text.

at the end of the energy scale above 4.5 Mev where the errors may be somewhat greater but certainly do not exceed ±10 kev at 5 Mev. The total widths are believed correct to within ±8% except where explicitly stated. The values of $\Gamma_p\Gamma_{p'}/\Gamma^2$ are estimated correct to within ±30%. Estimating the error in Γ_p/Γ is a matter of judgment with regard to possible improvement of the elastic scattering fit. What are judged to be the most probable values of Γ_p and $\Gamma_{p'}$ separately in view of uncertainties in Γ_p/Γ and $\Gamma_p\Gamma_{p'}/\Gamma^2$, subject to the requirement $\Gamma_p+\Gamma_{p'}=\Gamma$, are listed in columns 8 and 10. Resonance energies and widths are on the laboratory scale.

2.080-Mev Resonance

The assignment $J^\pi=\frac{1}{2}^+$ is unambiguous. This can be seen from the elastic fit and by comparison with the single-level curves of Fig. 2. The values of the parameters of the state must of course be obtained entirely from the elastic scattering data. The parameters of Table I are in essential agreement with those given by Val'ter et al.[7] and by Vorona et al.[9]

2.88-Mev Resonance

This broad shallow resonance is visible only at 90° and 165° in the elastic scattering cross section. As can be seen from the single-level curves of Fig. 2, only $J^\pi=\frac{1}{2}^-$ shows a dispersion shape at 165° and a peak at 90° with small effects at 39° and 125°. Results are in essential agreement with Vorona et al.[9]

3.095-Mev Resonance

This resonance is strong in the inelastic as well as the elastic scattering data. Without knowledge of the inelastic scattering partial width, the assignment from the elastic scattering data would be ambiguous. The peak at 165° and the absence of effect at 39° in the elastic scattering data suggest $\frac{5}{2}^-$ or $\frac{7}{2}^-$ with small Γ_p/Γ. Odd parity is also suggested by the 90° shape, which is unlike any single-level curve and must therefore show the effect of interference from the broad odd-parity 2.88-Mev resonance. The dip at 125°, where $P_2(\cos\theta)=0$, rules out $l=2$, and the shapes at all angles rule out $l=0$. A relative elastic scattering partial width

FIG. 4. The experimental differential inelastic c.m. scattering cross section for $Si^{28}(p,p')Si^{28*}$ ($Q=-1.78$ Mev) at $88°$ and $165°$ (laboratory) from 3.0 to 5.2 Mev. The curves are drawn through the points. The limits of error in the cross sections are discussed in the text.
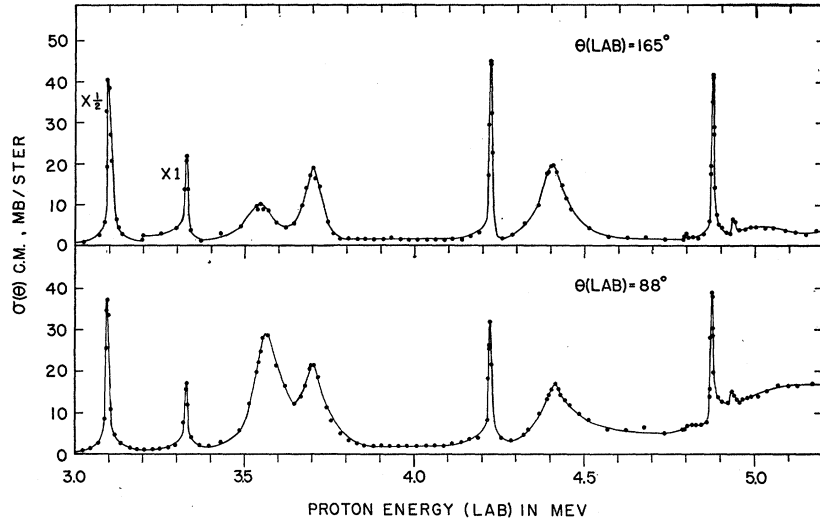
$\Gamma_p/\Gamma=0.2$ was used in the elastic fit with $J^\pi=\frac{5}{2}^-$. The inelastic scattering angular distribution is shown in Fig. 5. The curve is a theoretical distribution using $J^\pi=\frac{5}{2}^-$ and an outgoing channel spin mixture given by $\Gamma_{1\ 3/2}/\Gamma_{p'}=0.87$, and $\Gamma_{1\ 5/2}/\Gamma_{p'}=0.13$. The channel spin mixture was chosen to make the theoretical fit equal the least-squares fit. The values 0.2 for Γ_p/Γ and 0.24 for $\Gamma_p\Gamma_{p'}/\Gamma^2$ from the elastic and inelastic scattering fits are inconsistent with the requirement that $\Gamma_p+\Gamma_{p'}=\Gamma$. The possibility that Γ_p/Γ could be raised to about 0.3 is indicated by comparison of the fit with the experimental points at 165°, especially in view of the fact that a 3.7-kev target was used in taking the elastic scattering data. The values 0.3 for Γ_p/Γ and 0.21 for $\Gamma_p\Gamma_{p'}/\Gamma^2$ were used to compute Γ_p and $\Gamma_{p'}$ in columns 8 and 10 of Table I. Results are in agreement with Vorona et al.[9]

3.334-Mev Resonance

Comparison of the elastic scattering data with the theoretical shapes of Fig. 2 rules out all assignments but $J^\pi=\frac{3}{2}^+$ and $\frac{5}{2}^+$. Quantitative fit within the experimental error at all angles could only be achieved with $\frac{3}{2}^+$. $J^\pi=\frac{3}{2}^+$ with $\Gamma_p/\Gamma=0.70$ was used in the final elastic scattering fit of Fig. 3. In the inelastic angular distribution, shown in Fig. 6, the large experimental errors for $\theta_{c.m.}<60°$ were due to the necessity of subtracting a low-intensity background proton group from a target contaminent at this energy. In spite of these errors symmetry about 90° as previously assumed[9] is definitely ruled out. The curve of Fig. 6 is a theoretical fit to the angular distribution with $J^\pi=\frac{3}{2}^+$, $\Gamma_{0\ 3/2}=\Gamma_{p'}$, and $\Gamma_{2\ 5/2}=0$, taking into account interference from the $\frac{5}{2}^-$ state corresponding to the 3.095-Mev resonance with

TABLE I. Results of the analysis of the resonances in $Si^{28}(p,p)Si^{28}$ and $Si^{28}(p,p')Si^{28*}$. The columns $E_0(=E_0{}^{J\pi})$, J^π, l, $\Gamma(=\Gamma^{J\pi})$ and $\Gamma_p/\Gamma(=\Gamma_p{}^{J\pi}/\Gamma^{J\pi})$ contain the parameters used in the elastic scattering fit of Fig. 3. The next column contains the $\Gamma_p\Gamma_{p'}/\Gamma^2$ obtained from the fits to the inelastic scattering angular distributions. The last four columns contain the values of Γ_p and $\Gamma_{p'}$ considered most probable and the corresponding reduced widths expressed as a fraction of $3\hbar^2/2Ma$.

E_0 (Mev)	$E(P^{29*})$ (Mev)	J^π	l	Γ (kev)	Γ_p/Γ	$\Gamma_p\Gamma_{p'}/\Gamma^2$	Γ_p (kev)	$(2Ma/3\hbar^2)\gamma_p{}^2$	$\Gamma_{p'}$ (kev)	$(2Ma/3\hbar^2)\gamma_{p'}{}^2$
1.660[a, b]	4.326	$\frac{3}{2}^-$	1	(50)	1					
2.080	4.732	$\frac{1}{2}^+$	0	18.6(16.2c)	1		16.2	0.012		
2.88±0.02	5.50	$\frac{1}{2}^-$	1	400±60	1		400	0.22		
3.095	5.711	$\frac{5}{2}^-$	3	13.6(12.9c)	0.2	0.24	3.9	0.020	9.0	~1
3.334	5.942	$\frac{3}{2}^+$	2	9.4(8.4c)	0.7	0.13	6.4	0.0063	2.0	0.17
3.571	6.171	$\frac{3}{2}^-$	1	98	0.2	0.17	20	0.0067	78	~1
3.710	6.305	$\frac{1}{2}^-$	1	74	0.2	0.23	18	0.0056	56	0.8
3.98	6.57	$\frac{1}{2}^+$	0	200±20	1		200	0.041		
4.235	6.812	$\frac{3}{2}^+$	2	5.4(4.9c)	0.6	0.21	2.9	0.0016	2.0	0.004
4.36	6.93	$\frac{1}{2}^+$	0	120	1		120	0.022		
4.43	7.00	$\frac{1}{2}^-$	1	100	0.15	0.25	30	0.0068	70	0.1
4.884	7.438	$\frac{5}{2}^-$	3	8.6(8.4c)	0.3	0.25	2.9	0.0035	5.5	0.09
(5.4)	(7.9)	$(\frac{1}{2}^+)$	(0)	(300)	(1)					

[a] See reference 7.
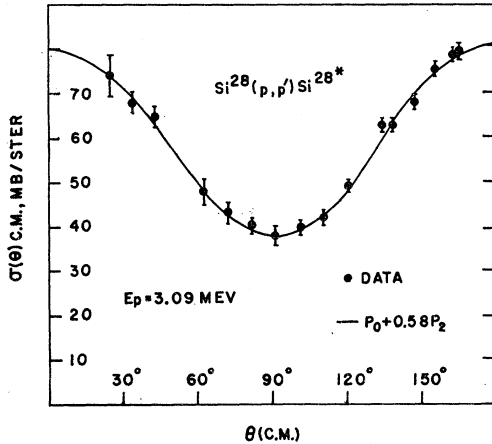[b] See reference 9.
c After correction for target thickness.

Fig. 5. Angular distribution of the inelastically scattered protons on resonance at 3.09 Mev. The curve $(P_0+0.58\ P_2)$ is the theoretical fit with $J^\pi=\frac{5}{2}^-$, $l'=1$ and the channel spin mixture given in the text.

the parameters given in the preceding paragraph and from the $\frac{3}{2}^-$ state corresponding to the 3.571-Mev resonance with the parameters given in the next paragraph. The assumption $\Gamma_2\ _{5/2}=0$ appears reasonable at this energy because of the barrier for protons with $l'=2$. If J^π were taken $\frac{5}{2}^+$ with $\Gamma_2\ _{3/2}=0$ and $\Gamma_0\ _{5/2}=\Gamma_{p'}$, a smaller term in P_1 would result. The least-squares fit is given by $P_0-0.29\ P_1-0.05\ P_2$.

3.571- and 3.710-Mev Resonances

From the elastic scattering data alone it would have been difficult or impossible to determine the locations, widths, and J^π of these two broad overlapping resonances, which were found to have a larger partial width for decay into the inelastic than into the elastic scattering channel. The total widths and resonance energies were determined from the inelastic scattering data with confirmation from the elastic scattering fit. The inelastic scattering angular distributions taken on the resonances and midway between them, shown in Fig. 7, are symmetrical about 90°, so that the interference terms must be even and the resonances must be due to states of the same parity. That the 3.571-Mev resonance can not be due to a state of even parity can be seen from the following: comparison of the elastic scattering shapes with the elastic scattering shapes of Fig. 2; the angular distribution at 3.57 Mev contains a large term in P_2 as expected of a $\frac{3}{2}^-$ state, while the angular distributions from even-parity states with $J\leqslant\frac{5}{2}$ would be expected to be isotropic using the lowest $l'(=0)$ for the $\frac{3}{2}^+$ and $\frac{5}{2}^+$ states; interference between this state and the even-parity state producing the 3.334-Mev resonance contributes a term in P_1 to the inelastic scattering angular distribution at 3.33 Mev. It then follows that the 3.710-Mev resonance can not be due to a $\frac{3}{2}^+$ state as previously postulated.[9] The elastic scattering shapes suggest $J^\pi=\frac{3}{2}^-$ or $\frac{1}{2}^-$. The inelastic scattering angular

distributions suggest $\frac{3}{2}^-$ at 3.571 Mev and $\frac{1}{2}^-$ at 3.710 Mev. With this combination successful elastic and inelastic scattering fits were achieved. At both resonances best elastic scattering fit was obtained with $\Gamma_p/\Gamma=0.2$. The curve at 3.57 Mev in Fig. 7 is the theoretical fit to the inelastic scattering angular distribution obtained with $l'=1$, $\Gamma_1\ _{3/2}=0.88\ \Gamma_{p'}$, and $\Gamma_1\ _{5/2}=0.12\ \Gamma_{p'}$; that at 3.71 Mev was obtained with $l'=1$, $\Gamma_1\ _{3/2}=\Gamma_{p'}$ and $\Gamma_3\ _{5/2}=0$. With this channel spin mixture and with interference included, the theoretical fit equaled the least-squares fit.

3.98-Mev Resonance

This broad resonance shows strongly in the elastic scattering data and is not apparent in the inelastic. $J^\pi=\frac{1}{2}^+$ is the only assignment that gives a reasonably good elastic scattering fit. $\Gamma_p/\Gamma=1$ in the fit of Fig. 3.

4.235-Mev Resonance

From Fig. 3 the elastic scattering shapes at 4.235 Mev are seen to be similar to those at 3.334 Mev. The only assignment giving a fit within experimental error at all angles was $J^\pi=\frac{3}{2}^+$. To explain the inelastic scattering angular distribution, shown in Fig. 8, there must be strong interference from a state of unlike parity. The only nearby resonance at which Γ_p/Γ is appreciably greater than zero is the broad resonance at 4.43 Mev most probably due to a state with $J^\pi=\frac{1}{2}^-$. The least-squares fit to the angular distribution at 4.23 Mev is given by

$$P_0-0.61\ P_1-0.28\ P_2.$$

The value of $\Gamma_p\Gamma_{p'}/\Gamma^2$ in Table I was calculated from the total cross section obtained by integrating the angular distribution. It is consistent within experimental error with $\Gamma_p=0.6\Gamma$ and $\Gamma_{p'}=0.4\Gamma$.
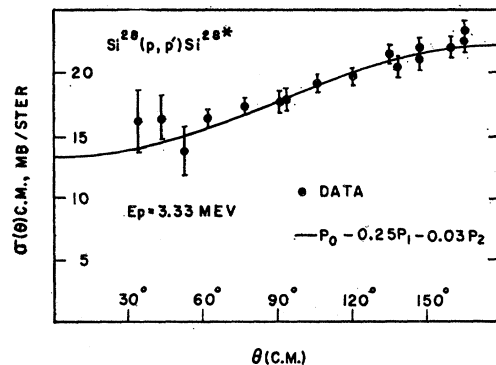

Fig. 6. Angular distribution of the inelastically scattered protons on resonance at 3.33 Mev. The curve $(P_0-0.25\ P_1-0.03\ P_2)$ is the theoretical fit with $J^\pi=\frac{3}{2}^+$, $l'=0$, the channel spin mixture given in the text and including interference from the negative-parity states corresponding to the 3.095- and 3.571-Mev resonances.
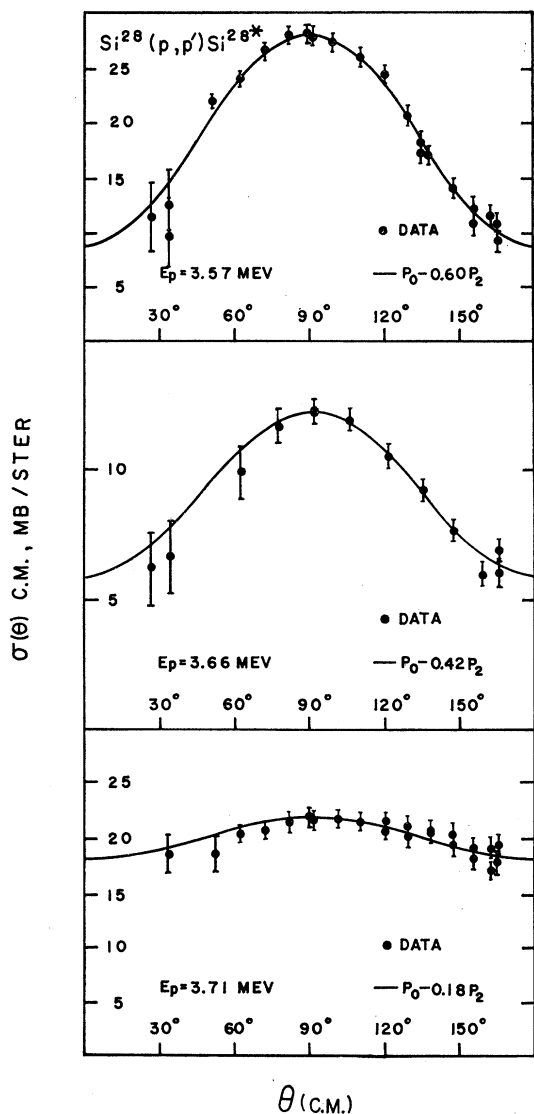
FIG. 7. Angular distributions of the inelastically scattered protons on resonance at 3.57 and 3.71 Mev and approximately midway between the resonances. The curves $(P_0-0.60\ P_2)$ at 3.57 Mev, $(P_0-0.42\ P_2)$ at 3.66 Mev and $(P_0-0.18\ P_2)$ at 3.71 Mev are the theoretical fits using $J^\pi=\frac{3}{2}^-$ and $\frac{1}{2}^-$ at 3.571 and 3.710 Mev, respectively, $l'=1$ at both resonances, the channel spin mixture given in the text and including mutual interference.

4.36-Mev Resonance

Like the resonance at 3.98 Mev, the 4.36-Mev resonance is apparent only in the elastic scattering cross section. The assignment $J^\pi=\frac{1}{2}^+$ is unambiguous.

4.43-Mev Resonance

The degree of isolation of this broad resonance in the inelastic scattering data is interesting in view of its proximity to the broad 4.36-Mev resonance in the elastic. As can be seen from the single-level shapes of Fig. 2, the effect of this resonance on the elastic scat-

tering cross section restricts the possible assignments to $\frac{3}{2}^-$ and $\frac{1}{2}^-$. Even with Γ_p/Γ as small as 0.15 the $\frac{3}{2}^-$ assignment gave a fit clearly not in agreement with the elastic scattering data. The magnitude of the P_1 term in the inelastic scattering angular distribution at 4.23 Mev is additional evidence for the $\frac{1}{2}^-$ assignment. The maximum value of $\Gamma_p\Gamma_{p'}/\Gamma^2$ for a two-channel reaction is entered for this resonance in Table I; a value somewhat exceeding this maximum was calculated from the total cross section obtained by integrating the angular distribution at 4.43 shown in Fig. 9. The elastic scattering data appear to allow a larger value of Γ_p/Γ than the 0.15 used in the fit of Fig. 3, so that the combination $\Gamma_p=0.3\Gamma$, $\Gamma_{p'}=0.7\Gamma$ is probably inside experimental error. The least-squares fit to the inelastic scattering angular distribution of Fig. 9 is given by

$$P_0-0.18\ P_1.$$

There is no difficulty in explaining the small term in P_1, since the inelastic scattering data show a broad resonance at or above 5 Mev which could be due to a state of even parity. Above 5 Mev there are known to be several broad resonances, at one of which even parity has been assigned.[10,12] The term in P_1 could also indicate that the $\frac{1}{2}^+$ state corresponding to the 4.36-Mev resonance has a small inelastic scattering partial width.

4.884-Mev Resonance

The assignment at this resonance like that at 3.095 Mev is $\frac{5}{2}^-$. This is immediately recognizable from the similarities between the 4.884-Mev and 3.905-Mev resonances in both the elastic and inelastic scattering cross sections. The slope in the inelastic scattering angular distribution, shown in Fig. 10, can be adequately explained by interference from a broad resonance at 5 Mev or above.

Additional Resonances at About 5 Mev

Two other narrow resonances were observed just below 5 Mev: one at 4.78 in both the elastic and
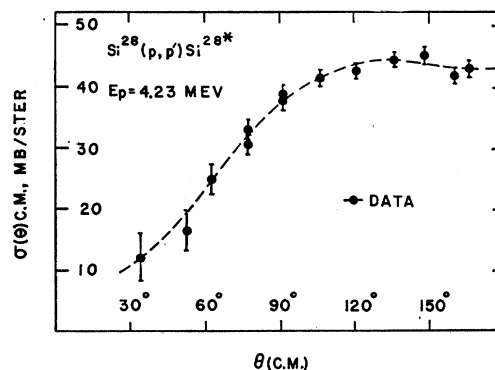

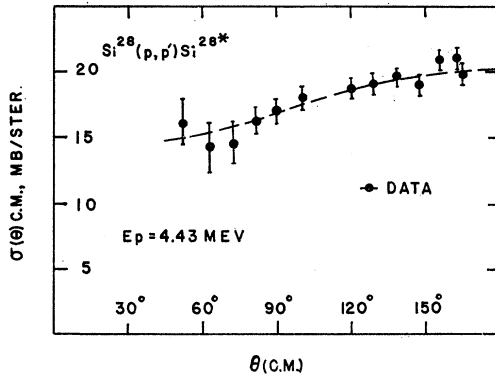FIG. 8. Angular distribution of the inelastically scattered protons on resonance at 4.23 Mev.

FIG. 9. Angular distribution of the inelastically scattered protons on resonance at 4.43 Mev.

FIG. 10. Angular distribution of the inelastically scattered protons on resonance at 4.88 Mev.

inelastic scattering data and one at 4.936 in the inelastic scattering data. Although the cross sections were small, these resonances were always seen in data taken in this region. It is impossible from the data to make assignments for the corresponding states. Significant improvement of the elastic scattering fit between 4.5 and 5 Mev was obtained by including a resonance at 5.4 Mev due to a $\frac{1}{2}^+$ state with the parameters given in Table I. This must probably be considered as additional evidence for a broad resonance above 5 Mev due to an even-parity state.

Partial and Reduced Widths

In columns 8 and 10 of Table I are listed values of the elastic and inelastic scattering partial widths which appear most nearly consistent with all three of the following: the value of Γ_p/Γ for the best elastic scattering fit; the value of $\Gamma_p\Gamma_{p'}/\Gamma^2$ obtained from the inelastic scattering cross sections; the requirement that $\Gamma_p+\Gamma_{p'}=\Gamma$. Columns 9 and 11 list the reduced elastic and inelastic scattering proton widths expressed as fractions of the Wigner limit $3\hbar^2/2Ma$, with $a=5.86$
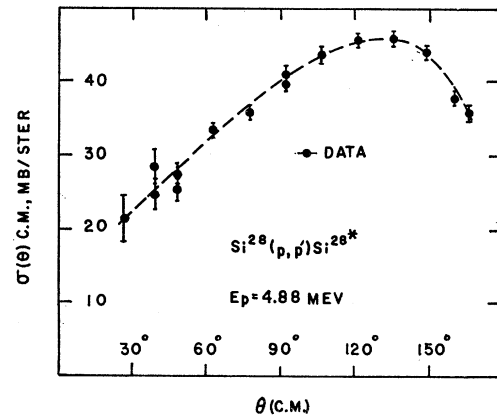
$\times 10^{-13}$ cm. The tables of Bloch $et\ al.$[17] were used to calculate the penetrability factors $A_l{}^2$ for the elastically scattered protons and the tables of Schiffer[18] for the inelastically scattered ones. The implications of the large inelastic scattered reduced widths are somewhat in question since the values listed as one at 3.095 and 3.57 Mev were actually calculated to be greater than one using the $A_{l'}{}^2$ from Schiffer's tables. This is perhaps not surprising in view of the uncertainties in the large magnitudes of the $A_{l'}{}^2$ introduced by uncertainties in the nuclear radius.

[17] I. Bloch M. H. Hull, Jr., A. A. Broyles, W. G. Bouricius, B. E. Freeman, and G. Breit, Revs. Modern Phys. 23, 147 (1951).
[18] J. P. Schiffer, Argonne National Laboratory Report ANL-5739 (unpublished).